Langmuir

Article

pubs.acs.org/Langmuir

Interactions of PAMAM Dendrimers with SDS at the Solid–Liquid Interface

Marianna Yanez Arteta,*[,†] Felix Eltes,[†] Richard A. Campbell,[‡] and Tommy Nylander[†]

[†]Department of Physical Chemistry, Lund University, P.O. Box 124, S-221 00 Lund, Sweden

[‡]Institut Laue-Langevin, 6 rue Jules Horowitz, BP 156, 38042 Grenoble Cedex 9, France

Supporting Information

ABSTRACT: This work addresses structural and nonequilibrium effects of the interactions between well-defined cationic poly(amidoamine) PAMAM dendrimers of generations 4 and 8 and the anionic surfactant sodium dodecyl sulfate (SDS) at the hydrophilic silica–water interface. Neutron reflectometry and quartz crystal microbalance with dissipation monitoring were used to reveal the adsorption from premixed dendrimer/surfactant solutions as well as sequential addition of the surfactant to preadsorbed layers of dendrimers. PAMAM dendrimers of both generations adsorb to hydrophilic silica as a compact monolayer, and the adsorption is irreversible upon rinsing with salt solution. SDS adsorbs on the dendrimer layer and at low bulk concentrations causes the expansion of the dendrimer layers on the surface. When the bulk concentration of SDS is increased, the surfactant layer consists of aggregates or bilayer-like structures. The adsorption of surfactant is reversible upon rinsing, but slight changes of the structure of the preadsorbed PAMAM monolayer were observed. The adsorption from premixed solutions close to charge neutrality results in thick multilayers, but the surface excess is lower when the bulk complexes have a net negative charge. A critical examination of the pathway of adsorption for the interactions of SDS with preadsorbed PAMAM monolayers and premixed PAMAM/SDS solutions with hydrophilic silica revealed that nonequilibrium effects are important only in the latter case, and the application of a thermodynamic model to such experimental data would be inappropriate.

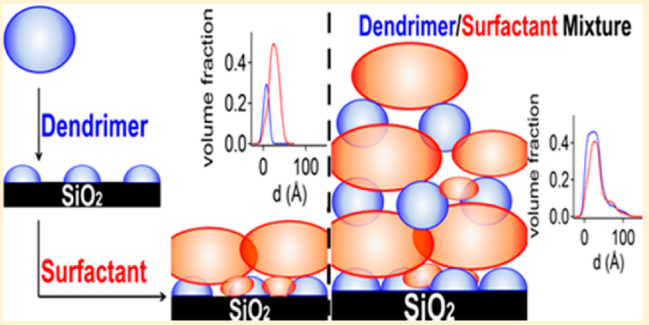

INTRODUCTION

Dendrimers are hyperbranched polymers with a well-defined architecture comprising three main components: an initiator core, branched interior shells, and exterior branches with surface groups that can be functionalized.[1] Their structure reflects the origin of the name, as in Greek "dendron" means "tree". Poly(amidoamine) (PAMAM) dendrimers were one of the first classes of dendritic polymers to be synthesized by Tomalia et al.[1] almost two decades ago. Since then, with their potential applications in, e.g., pharmaceuticals, in mind, they have been studied extensively.[2,3] PAMAM dendrimers are composed of an ethylendiamine or amine core and amidoamine branches with amine surface groups that have a pK_a of 8.0–9.2[4] and are therefore positively charged at neutral pH and below. PAMAM dendrimers can be modified to contain carboxylic surface groups that are negatively charged above pH 6–7. Since dendrimers can be functionalized relatively easily, their interactions with a range of molecules and surfaces can be controlled.

Dendrimers have an advantage in fundamental studies as a model of hyperbranched polymers. Controlled synthesis results in hierarchical structure and monodisperse polymers (typically with M_w/M_n falling in the range 1.000002–1.005). The iterative sequence reaction produces dendrimers which increase in size, molecular weight, and number of surface groups in each reaction step. The number of surface groups for PAMAM dendrimers increases as a function of the generation (G) by 2^{G+2}.[5] These dendrimers have a significantly more well-defined and symmetric structure compared to other polymeric architectures such as linear, cross-linked, and polydispersed branched. In this respect, they are more similar in shape and size to biological molecules, like globular proteins.[5]

Although PAMAM dendrimer synthesis is rather laborious and challenging for large-scale commercial applications, they have been investigated considering possible applications as gene vectors,[6] biosensors,[7] nanocapsules,[8] and many others. Of particular relevance for this work are previous studies on the interactions between PAMAM dendrimers and small amphiphilic molecules. However, most of these studies concern the bulk solution and surface behavior and do not provide detailed information on the mixed layer structure or the nonequilibrium aspects of the adsorption process. It has previously been shown that the anionic surfactant sodium dodecyl sulfate (SDS) does not bind significantly to anionic carboxylic acid terminated

Received: March 2, 2013
Revised: March 28, 2013
Published: April 4, 2013

   dx.doi.org/10.1021/la400774p | Langmuir 2013, 29, 5817–5831

dendrimers, while cationic surfactants such as alkyltrimethylammonium bromides show a strong attractive interaction.[9−11] On the other hand, cationic amine terminated dendrimers show the opposite behavior, as SDS interacts strongly with them especially at pH 7 and lower.[12−14]

Several models have been proposed for the interactions between oppositely charged surfactants and dendrimers in the bulk solution. Despite differences between the proposed models, most of them came to two important conclusions. First, the electrostatic interactions between the surface group of the dendrimers and the polar head of the surfactant play a major role in their association. Second, hydrophobic interactions between the hydrophobic tail of the surfactant and the PAMAM interior are also relevant, which is important given the potential for interactions with small hydrophobic drugs and their possible applications as drug delivery vehicles.[5]

Oppositely charged polyelectrolyte/surfactant (P/S) systems have numerous industrial applications such as detergency, paints, oil recovery, the food industry, and biotechnology, among others,[15] where their interfacial behavior is important. The adsorption of polyelectrolyte onto a solid surface often leads to reversal of the surface charge,[16−20] and thus ionic surfactants with the same charge as the bare surface adsorb to the polymer layer in spite of the electrostatic repulsion between the surfactant and the bare surface. As an example, the interactions of the polydispersed branched poly(ethylene imine) (PEI) with SDS at different interfaces have been studied extensively, and several models have been proposed to describe the effect of the solution conditions (pH and ionic strength among others).[18−21] In the absence of P/S interactions in the bulk solution, surfactant adsorption onto a polymer monolayer bound to a solid substrate can be reversible, partially reversible, or irreversible,[22] and the process can affect the structure of the preadsorbed polyelectrolyte monolayers, inducing swelling,[23] deswelling,[24] or desorption of the layer,[25] as a result of the change in the electrostatic interaction between the polyelectrolyte and the substrate. Although work has been carried out concerning the interaction of PAMAM dendrimers with surfactants and the interactions of dendrimers with surfaces, to our knowledge the interactions of PAMAM dendrimers and short-chain soluble surfactants have not been investigated at interfaces to date. Thus, contrary to the PEI/SDS system, there is no proposed interfacial model for well-defined branched polyelectrolytes interacting with surfactants.

Oppositely charged P/S systems are known to interact strongly in the bulk leading to associative phase separation around bulk compositions corresponding to the charge neutrality of the complexes and aggregates; yet, the interfacial properties of the systems are known to determine the performance in many commercial applications.[26] Generally, the maximum surface excess coincides with this phase separation region, although the specific effects of bulk aggregates on the structure and composition of the surface layers are not fully understood.[26] The importance of understanding how the bulk interactions affect the surface properties was addressed by Dedinaite et al.[27] who compared the interactions of SDS with preadsorbed layers of poly((propionylolxy)ethyl)trimethylammonium chloride (PCMA) at the mica−water interface and the interactions of PCMA/SDS bulk aggregates with the substrate. They showed that the mixed adsorption layers of aggregates at the mica interface were trapped in metastable states and that true equilibrium was not reached under the experimental conditions used.

The aim of the present study is to gain a comprehensive understanding of the interactions at surfaces of well-defined hyperbranched polymers and oppositely charged surfactants, with particular emphasis on nonequilibrium aspects. PAMAM dendrimers are chosen as the model polyelectrolyte in this work due to their low polydispersity. Given the strong interactions of these components manifested as associative phase separation in the bulk, it is necessary to consider whether or not the interfacial layers formed are at equilibrium. Therefore, we have conducted three sets of experiments. The first set of experiments is dedicated to the adsorption of PAMAM dendrimers on silica, followed by the interaction of the preadsorbed PAMAM monolayer with pure SDS solutions of different concentrations added sequentially (without PAMAM in the bulk), and an examination of the reversibility of these interactions. The second set addresses the formation of layer structures from premixed PAMAM G4/SDS at different complex charge ratios. A range of bulk compositions, from positive to negatively charged dendrimer/SDS bulk complexes, are considered to assess how the formation of kinetically trapped particles in the bulk affects the resulting surface structures. Finally, the third set considers differences in the interfacial layers of PAMAM and SDS which have experienced a different sample history. These measurements were carried out both by direct (single) and sequential (multiple) additions of both surfactant to preadsorbed PAMAM layers and premixed PAMAM/SDS solutions. These data allow us to discuss the equilibrium state of the system and the applicability of a thermodynamic model to the experimental data.

The work was carried out using a combination of quartz crystal microbalance with dissipation monitoring (QCM-D) and neutron reflectometry (NR) measurements. QCM-D allows monitoring the adsorption process at the solid−water interface in real time with a sensitivity in the 0.01 mg m^{-2} range,[28] and gives information both about the total surface excess, i.e., adsorbed matter and entrapped water, and about the viscoelastic properties of the adsorbed layers. NR gives information about the interfacial structure and composition through the fitting of neutron reflectivity profiles of interfacial layers with equivalent chemical composition but different isotopic composition.[29] This was achieved by selective deuteration of the surfactant and the solvent as has been applied successfully in previous studies.[17,30]

EXPERIMENTAL SECTION

Materials and Sample Preparation. Deionized water, passed through a purification system (Milli-Q, resistivity = 18.2 mΩ.cm, organic content = 4 ppb), and/or D_2O (Euroiso-top, C. E. Saclay, France) were used for the preparation of the samples. Poly(amidoamine) dendrimer (PAMAM, Sigma-Aldrich) with ethylendiamine core, generation 4.0 (G4, 10 wt % in methanol) and 8.0 (G8, 5 wt % in methanol), were used without any further purification. Some relevant physical properties of the dendrimers used are summarized in Table 1. All the dendrimer samples in methanol were dried in a vacuum oven for 1 day before dissolution in the appropriate aqueous solvent. Aqueous solutions of PAMAM dendrimer were stored at 4 °C and were prepared a maximum of two weeks prior to the measurements. Sodium chloride (NaCl, Suprapure 99.99%) was obtained from Merck and was used as received. The aqueous solution had a constant ionic strength, by adding 10 mM NaCl and adjusting the pH to 7.2−7.4 with small aliquots of concentrated hydrochloric acid (Merck, for analysis 37%) or sodium hydroxide (Sigma-Aldrich). Hydrogenated sodium dodecyl sulfate (hSDS, BDH Chemicals Ltd. 99%) was recrystallized two times in ethanol (Kemetyl AB 99.5%). A hot filtration process was carried out to remove insoluble impurities,

dx.doi.org/10.1021/la400774p | Langmuir 2013, 29, 5817−5831

Table 1. Physical Properties of Generations 4 and 8 of PAMAM Dendrimers

generation	theoretical molecular weight[a] (g mol^{-1})	hydrodynamic radius[b] (Å)	surface groups[c]	density[d] (g cm^{-3})	molecular volume[e] (Å^3)
4	14215	24.5	64	1.224	19290
8	233383	66.3	1024	1.231	314900

[a]Theoretical molecular weight of the dendrimers as reported by the manufacturer. [b]Values of the hydrodynamic radius of the dendrimers taken from Ainalem et al.[31] [c]Surface groups represent the maximum number of amino groups in the periphery of the dendrimer. [d]Density of the dendrimers was extracted from Betley et al.[32] [e]Density was used for the calculations of the molecular volumes employing the theoretical molecular weight and compared with other references.[3,32,33]

and each time, the solutions were cooled over several hours to ensure the purity of the crystallized surfactant. Deuterated SDS (dSDS, Cambridge Isotopes, 99%) was used as received.

Electrophoretic Mobility Measurements. Electrophoretic mobility (EM) measurements were performed to obtain the charge of the PAMAM dendrimer/SDS complexes in a mixture. The mixtures were prepared immediately before the measurement according to the standard mixing protocol.[34] Solutions of the same volume of PAMAM and SDS were prepared with a concentration twice the intended final concentration and they were poured simultaneously in a beaker immediately before each measurement. This procedure was employed in order to minimize the amount of kinetically trapped aggregates.[35]

EM measurements were conducted employing the M3-PALS technique (Phase analysis Light Scattering), using a zetasizer Nano ZS (Malvern Instruments Ltd., Worshestershire, UK). An electric field was applied to the solutions, which made the complexes travel toward an electrode with a certain velocity depending on their charge and size. The EM value reported for each sample corresponds to the average of 5 measurements.

Quartz Crystal Microbalance with Dissipation Monitoring Measurements. QCM-D measurements were performed using an E4 system (Q-Sense, Gothenburg, Sweden). The principle of the technique has been described elsewhere.[36] The experimental setup consists of four flow cell modules, each with one sensor and a sample volume of 0.5 mL, which can be measured simultaneously. The temperature was 23 °C for all QCM-D measurements. The flow of solutions through each module was controlled with a peristaltic pump (Ismatec IPC-N 4, Zürich, Switzerland) at a flow rate of 0.7 mL min^{-1} for approximately 2−5 min. The quartz crystals used in the experiments have a fundamental frequency of 4.95 MHz and are coated with a SiO_2 layer (QSX 303, Q-Sense). The crystals were rinsed prior to and after their use with Milli-Q water and ethanol, blown dry with nitrogen, plasma cleaned for 5−10 min (Harrick Scientific Corp, model PDC-3XG, New York, USA), and stored in 2% SDS solution or ethanol for a minimum of 30 min. Each crystal was placed in a flow module immediately after plasma-cleaning, and then 10 mM NaCl pH 7 solution was flowed through the cells. The fundamental frequencies (f) and corresponding energy dissipation factors (D) of the odd overtones 1 to 13 were measured for each crystal before each experiment, and a stable baseline was ensured before the exposure of solutions containing surface-active material to the silica surface.

QCM-D Data Evaluation. A shift of the resonance frequency of the crystal (Δf) occurs due to a change in the adsorbed amount of material (Δm). For a rigid layer, evenly distributed and small enough compared to the weight of the crystal ($\Delta f/f \ll 1$), the mass varies linearly according to the Sauerbrey equation:[36]

$$\Delta m = -\frac{C}{n}\Delta f \tag{1}$$

where C is a proportionality constant (C is approximately 17.7 ng s cm^{-2} for a 5 MHz crystal) and n is the overtone number. In a QCM-D experiment, the solvent associated with the adsorbed layer also contributes to the frequency change; therefore, the quantity Δm is usually referred to as the "wet mass". With changes in density or viscosity of the bulk liquid or the adsorbed layer, the linear relation between the adsorbed mass and the frequency shift is not necessarily valid. For viscoelastic films, the additional energy dissipation and frequency overtone-dependent change can be modeled employing the so-called Voigt-based representation.[28,37] In this model, the adsorbed film is represented by a frequency-dependent complex shear modulus G:

$$G = G' + iG'' = \mu_f + i2\pi f\eta_f = \mu_f(1 + i2\pi f\tau_f) \tag{2}$$

where μ_f is the elastic shear modulus, η_f the shear viscosity, and τ_f the characteristic relaxation time of the film. The frequency and dissipation changes are related to the viscoelastic properties of the adsorbed film:

$$\Delta f = \mathrm{Im}\left(\frac{\beta}{2\pi t_q \rho_q}\right) \tag{3}$$

and

$$\Delta D = -\mathrm{Re}\left(\frac{\beta}{\pi t_q \rho_q}\right) \tag{4}$$

where β is a function of the thickness and density of the adsorbed film and of the density and viscosity of the bulk liquid. The expression for β can be found in the Supporting Information.

The experimental QCM-D data were modeled using the Sauerbrey expression and the Voigt-based representation with the software QTools (Q-Sense, Gothenburg, Sweden) employing experimental data from the third, fifth, seventh, and ninth overtones. These overtones were chosen because on lower harmonics energy trapping is insufficient and on higher harmonics side bands interfere with the main resonance.[38] Both models give similar values when ΔD is lower than 1×10^{-6} (in agreement with literature[39]) but the Sauerbrey expression becomes insufficient at higher values and for frequency overtone-dependent changes. The parameters used in the Voigt-based models are summarized in the Supporting Information.

Neutron Reflectometry Measurements. NR measurements were recorded using the time-of-flight reflectometer FIGARO at the Institut Laue-Langevin (Grenoble, France).[40] The instrument was used with a chopper pair giving neutron pulses with a wavelength resolution of 4% in the range 2−30 Å. Data acquisitions were carried out at fixed incident angles of 0.62° and 3.8°. The neutron reflectivity profiles presented are the intensity ratios of incoming and reflected neutron intensity in the specular reflection, corrected for background scattering, to those in the incident beam as a function of the momentum transfer, Q, defined by

$$Q = \frac{4\pi \sin\theta}{\lambda} \tag{5}$$

where θ is the angle of incidence and λ is the wavelength. The measurements were performed using two different surfactant isotopic contrasts, hSDS and dSDS, and three different solvent isotopic contrasts, D_2O (scattering length density 6.36×10^{-6} Å^{-2}), H_2O (scattering length density -0.56×10^{-6} Å^{-2}), and a mixture of D_2O and H_2O in a 0.38 D_2O volume fraction to contrast match the scattering length density of silicon (cmSi, scattering length density 2.07×10^{-6} Å^{-2}). Two different modes of carrying out the adsorption study were employed, sequential addition of SDS onto preadsorbed PAMAM monolayers and adsorption of PAMAM/SDS mixtures on silica. The average acquisition times for the former approach were 1 h for D_2O, 1.25 h for H_2O, and 1.5 h for cmSi solvent contrasts. For the latter method of addition, sequential scans were recorded during a period of approximately 4−5 h until the data showed that the interfacial layers were not changing significantly between each measurement.

Liquid flow cells with an internal volume of ~2 mL were employed for all the NR experiments where the liquid was located below the silicon crystal.[40] The scheme of NR experiments at the solid−liquid interface has been described elsewhere.[41] Silicon crystals (dimensions l

dx.doi.org/10.1021/la400774p | Langmuir 2013, 29, 5817−5831

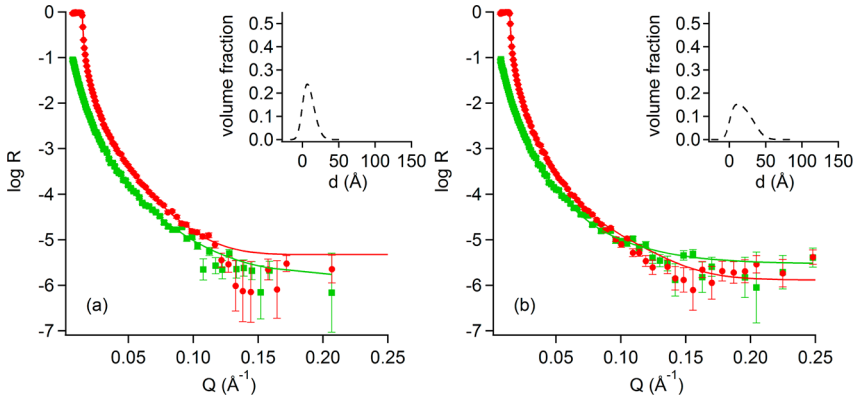

Figure 1. Neutron reflectivity profiles for the adsorption of PAMAM (a) G4 and (b) G8 onto hydrophilic silica. The solvent contrasts used to characterize the layers were D_2O (red) and H_2O (green). The lines correspond to the calculated model. The insets correspond to the volume fraction of dendrimer (black dashed line) as a function of the distance (d) to the surface (SiO_2).

$\times w \times h$ of 80 × 50 × 10 mm^3) with a SiO_2 layer (≈10 Å) were used as a substrate. The crystals were freshly polished (Siltronix, France) and cleaned using a dilute piranha solution composed of water, sulfuric acid (Merck, for analysis 95−97%), and hydrogen peroxide (Merck, for analysis 30%) in a 5:4:1 volume ratio for 20 min at 80 °C. For every solution exchange, about 20 mL of solution was injected through the cell to ensure the very efficient exchange of the bulk solution.

NR Data Evaluation. The NR data were fitted using the software Motofit,[42] based on the interaction of neutrons with a stratified layer model and using the Abeles matrix method.[43] The parameters to fit for each layer were the thickness (d), the scattering length density (ρ), the solvent volume fraction ($\nu_{solvent}$), and the roughness (δ). The silica layer of one of the silicon crystals was characterized in the three isotopic contrasts of the solvent to determine the appropriate values of d, $\nu_{solvent}$, and δ. In our experience, it was then sufficient to characterize the silica layer of the others freshly polished crystals only in D_2O to check for surface contamination. More information about the silica layer characterization can be found in the Supporting Information. The dendrimer monolayers adsorbed on silica were characterized in H_2O and D_2O. In the experiments with preadsorbed dendrimers and sequential additions of SDS, the interactions were characterized with the surfactant contrasts hSDS and dSDS in separated cells to ensure that the surfactant layers do not contain isotopic mixtures. In this case, solvent exchange was performed in each cell: D_2O for hSDS and H_2O and cmSi for dSDS. In the premixed PAMAM/SDS experiments, each isotopic contrast (hSDS/D_2O, dSDS/H_2O, and dSDS/cmSi) was measured in different cells because the layers were insufficiently stable to rinsing to perform the solvent exchange method.

The silica substrate was modeled as one layer in three regions (Si−SiO_2 layer−solvent). The adsorption of the polymer was modeled as two layers in four regions (Si−SiO_2 layer−PAMAM−solvent). It should be noted that specular reflections provide information on the density in the direction perpendicular to the surface over a large area and are therefore not sensitive to lateral inhomogeneities on the scale of the dendrimer size. This is due to the fact that the inhomogeneities are much smaller than the coherence length of the neutron measurements (tens of micrometers). We always employed a model with minimal number of layers to fit the experimental data, e.g., a one-layer model was use to model the adsorbed PAMAM layer, in order to obtain best fit to the experimental data with minimal number of fitting parameters. The roughness of the silica layer lies in the range 1−5 Å (see table in Supporting Information). As the dendrimer or dendrimer/surfactant layers adsorb they spread to maximize the contact points with the surface. The NR fitting parameters show that the roughness between the surface and the adsorbed layers does not increase compared to that of the bare substrate.

Although the scattering length densities of most materials can be calculated with the molecular composition and volume, it has been shown that PAMAM dendrimers exchange some protons for deuterium,[33] therefore the scattering length density of the dendrimer layer was also used as a fitting parameter (see table in Supporting Information). The reflectivity curves for the addition of SDS onto preadsorbed monolayers of PAMAM and the adsorption of premixed PAMAM-G4/SDS solutions on silica were modeled as mixed dendrimer/surfactant layers (Si-SiO_2 layer-Adsorbed Layer 1-Adsorbed Layer 2-...-solvent) and the number of layers depended of the system. For the mixed layers, the volume fractions (ν) of dendrimer, surfactant, and solvent were calculated from the respective scattering length density in each contrast:

$$\nu_{dendrimer}\rho_{dendrimer} + \nu_{surfactant}\rho_{surfactant} + \nu_{solvent}\rho_{solvent} = \rho_{layer} \quad (6)$$

The volume fraction of each component in each layer was solved using the different scattering length densities fitted for each of the three isotopic contrasts measured. The contrasts were treated independently to give a common model that fitted the experimental data. The global fitting algorithm in Motofit was not employed, as experiments in different cells can cause slightly different surface coverage, so the errors associated to the parameters correspond to the standard deviation between the parameters of different models.

The surface excess (Γ) of each compound was calculated using the following equation:

$$\Gamma = \frac{d \cdot \nu \cdot M}{V_M \cdot N_A} \quad (7)$$

where M and V_M are the molar mass and molecular volume of the component, respectively, and N_A is Avogadro's number. The scattering length density of the different species in any given layer can be found in the Supporting Information.

RESULTS AND DISCUSSION

Interaction of SDS with Preadsorbed Layers of PAMAM. *Adsorption of PAMAM Dendrimers onto Hydrophilic Silica.* PAMAM dendrimer solutions, of concentrations 100 and 108 ppm for PAMAM-G4 and PAMAM-G8, respectively, were exposed to hydrophilic silica surfaces. The concentrations were chosen to obtain the same number of positive charges in both types of dendrimer solutions. The adsorption of these polyelectrolytes is fast and steady state surface excess is reached within a few minutes; nevertheless, for all measurements, the systems were allowed to equilibrate for 30 min before rinsing with salt solution. A slight desorption of both investigated generations of dendrimers from the silica surface during rinsing with a 10 mM NaCl solution was observed. Ainalem et al.[33] made a similar observation under similar solvent conditions, although they used NaBr instead of NaCl. Further rinsing did not cause additional desorption of

dx.doi.org/10.1021/la400774p | Langmuir 2013, 29, 5817−5831

Table 2. Parameters Obtained from the Modeling of the NR Profiles, Calculated Total Mass (m_{total}), and Number of Surfactant Molecules Per Polymer Molecule for the Adsorption of SDS onto a Pre-Adsorbed PAMAM-G4 Monolayer on Silica[a]

C_{SDS} (mM)	layers	d (Å)	δ (Å)	$v_{dendrimer}$	$v_{surfactant}$	$n_{surfactant}/n_{dendrimer}$	m_{total} (mg m^{-2})
0	Layer 1	13.5 ± 0.1	4 ± 1	0.35 ± 0.03	-	-	1.5 ± 0.1
0.20	Layer 1	24 ± 1	5 ± 2	0.20 ± 0.02	0.06 ± 0.02	14 ± 6	3.5 ± 0.2
	Layer 2	8 ± 2	3 ± 1	-	0.31 ± 0.08	-	
0.66	Layer 1	24 ± 1	5 ± 1	0.20 ± 0.02	0.09 ± 0.02	23 ± 6	3.5 ± 0.2
	Layer 2	9 ± 2	3 ± 1	-	0.34 ± 0.09	-	
2.1	Layer 1	14.1 ± 0.2	6 ± 3	0.34 ± 0.02	0.16 ± 0.02	23 ± 3	4.4 ± 0.2
	Layer 2	25 ± 2	7 ± 2	-	0.4 ± 0.1	-	
6.7	Layer 1	14.4 ± 0.5	6 ± 3	0.33 ± 0.01	0.14 ± 0.01	20 ± 1	4.4 ± 0.5
	Layer 2	26 ± 4	7 ± 2	-	0.5 ± 0.1	-	
Rinse test	Layer 1	15.5 ± 0.2	5 ± 2	0.28 ± 0.01	-	-	1.6 ± 0.1

[a]The roughness (δ) values correspond to the roughness with the adjacent layer or the subphase. The errors correspond to the calculated standard deviation between the different values for the parameter in the best fitting of each contrast. The total mass corresponds to the surface excess of dendrimer and surfactant and the mass of solvent.

Table 3. Parameters Obtained from the Modeling of the NR Profiles, Calculated Total Mass (m_{total}), and Number of Surfactant Molecules Per Polymer Molecule for the Adsorption of SDS onto a Pre-Adsorbed PAMAM-G8 Monolayer on Silica[a]

C_{SDS} (mM)	layers	d (Å)	δ (Å)	$v_{dendrimer}$	$v_{surfactant}$	$n_{surfactant}/n_{dendrimer}$	m_{total} (mg m^{-2})
0	Layer 1	33 ± 6	12 ± 4	0.16 ± 0.03	-	-	3.4 ± 0.6
0.20	Layer 1	37 ± 3	3 ± 1	0.08 ± 0.01	0.15 ± 0.02	1436 ± 152	7.3 ± 0.3
	Layer 2	26 ± 1	6 ± 1	0.08 ± 0.01	0.05 ± 0.02	201 ± 93	
	Layer 3	7 ± 1	3 ± 1	-	0.08 ± 0.05	-	
0.66	Layer 1	36 ± 2	6 ± 2	0.08 ± 0.01	0.21 ± 0.01	2159 ± 236	8.7 ± 0.3
	Layer 2	30 ± 2	4 ± 1	0.08 ± 0.01	0.08 ± 0.02	381 ± 116	
	Layer 3	15 ± 1	4 ± 1	-	0.06 ± 0.01	-	
2.1	Layer 1	36 ± 1	5 ± 2	0.08 ± 0.01	0.26 ± 0.01	2618 ± 102	9.3 ± 0.5
	Layer 2	31 ± 4	5 ± 2	0.08 ± 0.01	0.13 ± 0.02	615 ± 211	
	Layer 3	19 ± 2	5 ± 2	-	0.08 ± 0.03	-	
6.8	Layer 1	39 ± 7	1 ± 1	0.06 ± 0.01	0.31 ± 0.06	3794 ± 613	12.7 ± 0.2
	Layer 2	41 ± 2	4 ± 1	0.06 ± 0.01	0.20 ± 0.01	1272 ± 32	
	Layer 3	35 ± 5	10 ± 3	-	0.09 ± 0.04	-	
Rinse test	Layer 1	28 ± 1	12 ± 4	0.22 ± 0.01	-	-	2.9 ± 0.1

[a]The parameters are described in the footnote of Table 2.

the polyelectrolytes and the data recorded after rinsing are those reported.

The parameters extracted from fitting the NR profiles (see Figure 1) and the calculated surface excesses are presented in Tables 2 and 3. The values for the total surface excess of dendrimer plus solvent, 1.5 ± 0.1 and 3.4 ± 0.6 mg m^{-2} for PAMAM-G4 and PAMAM-G8, respectively, are consistent with the QCM-D data (see full line arrows in Figure 2), where the surface excesses are 1.4 ± 0.1 and 3.7 ± 0.2 mg m^{-2}. It has been observed that the dendrimer surface excess is determined by the balance between the electrostatic attraction to the oppositely charged surface that cause a deformation of the dendrimer structure and the lateral repulsion between dendrimer molecules.[33] This is also found in the present study, where PAMAM-G8, with approximately 1024 charges per molecule, occupy a smaller volume fraction of the adsorbed layer compared to PAMAM-G4, which we attribute to the larger electrostatic lateral repulsion.

Both PAMAM-G4 and G8 adsorb on silica as a thin compact monolayer and both have a high solvent content (65% and 84% for PAMAM-G4 and PAMAM-G8 respectively). Previous work has shown that the dendrimer structures are hydrated in bulk solution and the hydration corresponds to a solvent volume fraction of 0.49 ± 0.04 as estimated from SANS studies of PAMAM-G4 dendrimers,[3] while simulations of hydration at neutral pH conditions gave a lower average water content, corresponding to a volume fraction of approximately 0.28 ± 0.06.[44] For higher PAMAM generations, the average volume

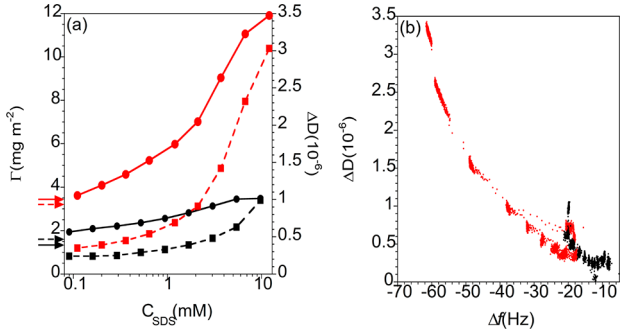

Figure 2. (a) Surface excess (Γ, circles and full line) obtained from modeling of the QCM-D data and dissipation change (ΔD, squares and dashed line) as a function of the SDS concentration and (b) dissipation change (ΔD) as a function of the frequency change (Δf) for the addition of SDS to preadsorbed PAMAM-G4 (black) and PAMAM-G8 (red) monolayers on silica. The arrows in (a) represent the surface excess before the addition of surfactant (full line) and after diluting with solvent (dashed line) to the preadsorbed monolayers. Lines are only to guide the eye. The frequency versus dissipation changes correspond to the overtone 5.

dx.doi.org/10.1021/la400774p | Langmuir 2013, 29, 5817−5831

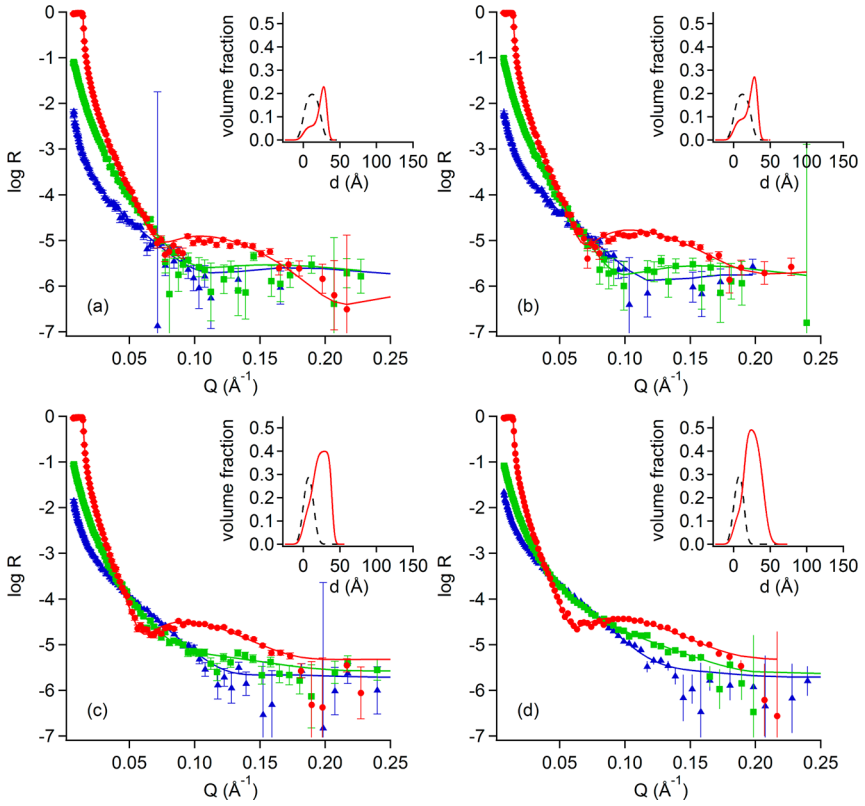

Figure 3. Neutron reflectivity profiles for the adsorption of (a) 0.20, (b) 0.66, (c) 2.1, and (d) 6.7 mM SDS onto a preadsorbed PAMAM-G4 monolayer on hydrophilic silica. The solvent contrasts used to characterize the layers were hSDS/D_2O (red), dSDS/H_2O (green), and dSDS/cmSi (blue). The lines correspond to the calculated model. The insets correspond to the volume fraction of dendrimer (black dashed line) and surfactant (red line) as a function of the distance (d) to the surface (SiO_2).

fraction of the dendrimer hydration water is slightly reduced according to SANS measurements.[3] If the hydration of each dendrimer molecule is taken into account, the effective polymer surface coverage is larger in terms of hydrated polymer molecules per unit area. Even if we correct for this fact, the dendrimers in the present study are not as closely packed on the surface as has been observed in previous AFM studies.[45] The thickness of the polyelectrolyte monolayers obtained from QCM-D and NR modeling for both generations is 73−75% smaller than their reported hydrodynamic diameter, which is consistent with previous results.[33,46] Bliznyuk et al.[46] showed experimentally that the thicknesses of PAMAM dendrimer monolayers at the silica−water interface were approximately 60−70% less than the average diameter of the dendrimer, and they concluded that the dendrimers are flattened rather than collapsed. Longtin et al.[47] showed that PAMAM dendrimers of generations above 4 adsorb irreversibly, within an experimentally accessible time scale, onto hydrophilic silica at high pH (above 6) and low ionic strength (below 0.1 M KCl). This was ascribed to the fact that the dendrimers spread on the surface and the strongly deformed and flattened molecules with many contact points with the substrate desorb only slowly after replacing the polymer solution with solvent (rinsing).[47,48] Similar behavior has been reported for the adsorption of PAMAM dendrimers of different generations onto mica[45] and carboxylic acid-terminated monolayers linked to silicon surfaces.[49]

Interactions of SDS with Preadsorbed PAMAM Monolayers on Hydrophilic Silica. The preadsorbed PAMAM dendrimer monolayers on hydrophilic silica after rinsing were exposed to sequential additions of SDS solutions of increasing bulk concentrations. These experiments were designed specifically to reveal PAMAM/SDS interactions at the surface, hence there was no additional PAMAM present in the bulk solutions. At a pH value slightly above 7 the dendrimers have a positive charge that is mainly located on the terminal primary amines,[50] and due to their hyperbranched architecture not all of these amine groups can be in contact with the hydrophilic silica surface. Therefore, adsorption of the polyelectrolyte is expected to lead to charge reversal of the silica surface, which enables the adsorption of oppositely charged surfactant, as has been observed for PEI/SDS.[18,19]

Initially, QCM-D experiments were carried out, and the first additions of low bulk concentrations of SDS result in a decrease in frequency of the crystals (raw data may be found in the Supporting Information), which corresponds to an increase of the surface excess that must be due to surfactant adsorption. Figure 2a shows the total surface excess calculated from the frequency and dissipation shift after the adsorption of SDS to the preadsorbed PAMAM monolayers and the dissipation change as a function of the bulk surfactant concentration. The total surface excess for the PAMAM-G8 system is higher for all the SDS concentration range studied compared to the PAMAM-G4 case. This difference can be rationalized by considering that the larger PAMAM-G8 have a higher number of charged groups exposed on its surface, which allows electrostatic interactions with more surfactant molecules compared to the smaller dendrimer generation. We will discuss this point further below based on the NR data, which allow the

dx.doi.org/10.1021/la400774p | *Langmuir* 2013, 29, 5817−5831

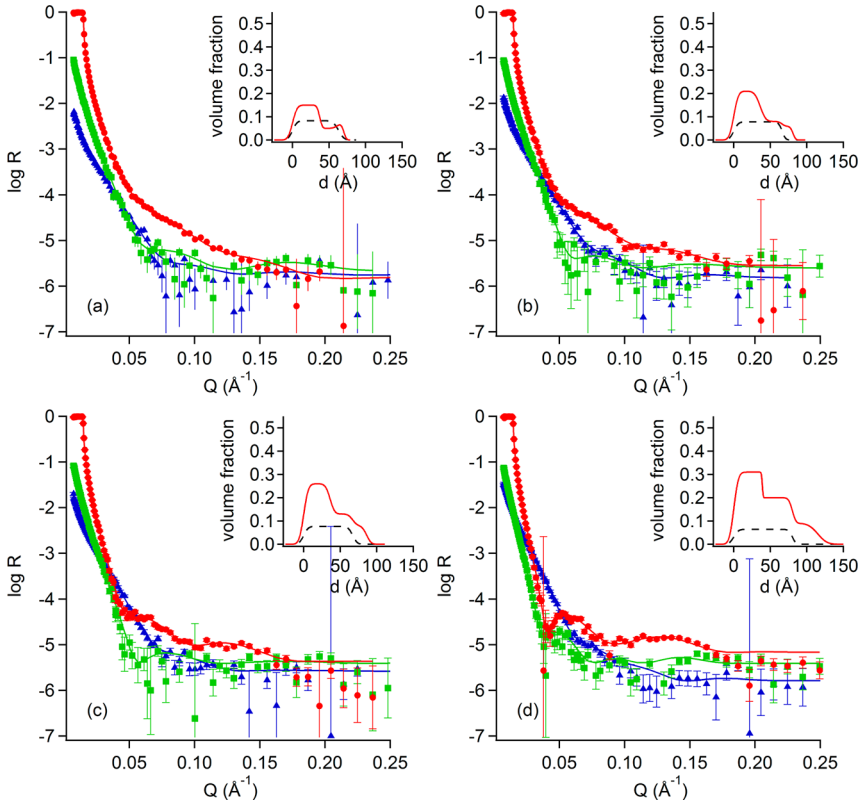

Figure 4. Neutron reflectivity profiles for the adsorption of (a) 0.20, (b) 0.66, (c) 2.1, and (d) 6.7 mM SDS onto a preadsorbed PAMAM-G8 monolayer on hydrophilic silica. The solvent contrasts used to characterize the layers were hSDS/D_2O (red), dSDS/H_2O (green), and dSDS/cmSi (blue). The lines correspond to the calculated model. The insets correspond to the volume fraction of dendrimer (black dashed line) and surfactant (red line) as a function of the distance (d) to the surface (SiO_2).

determination of the dendrimer/surfactant ratio and structure in the adsorbed layer.

Figure 2b shows the frequency vs the dissipation change for the interactions of SDS with a preadsorbed monolayer of PAMAM on hydrophilic silica, which provides additional information about the adsorption process. As the frequency is related to the surface excess, this plot may also be interpreted as a relation between the surface excess and the dissipation parameter. The highest frequency values (closest to zero) are related to the lowest surface excess where there is only a monolayer of dendrimer adsorbed. Here, the dendrimer adopts a very flat conformation and thus a low dissipation. As the PAMAM monolayers are exposed to higher concentrations of SDS (again, raw data may be found in the Supporting Information), the frequency shift does not change linearly with the change in dissipation. The interactions of surfactant molecules with the polymer layer are observed as the frequency shift becomes more negative (increase in surface excess). Initially, for both generations of dendrimers, the dissipation does not change very much or it even decreases slightly with decreasing frequency shift. This indicates the formation of a slightly more rigid interfacial layer compared to the bare dendrimer monolayer. These layers are not very viscous and the adsorption of monomeric SDS on the polymer is likely to be driven by both electrostatic and hydrophobic strong interactions. When the dendrimer monolayers are exposed to SDS solutions with concentrations higher than approximately 1.0 and 0.64 mM for PAMAM-G4 and PAMAM-G8, respectively, the dissipation increases indicating more viscous layers (Figure 2a). Two different slopes can be identified in this region. The region with the less steep slope, that occurs at intermediate bulk surfactant concentrations from approximately 1.0 to 5.5 mM, is related to changes in the structure and composition of the adsorbed layers. Conformational changes are likely to be due to a change in the nature of the interactions where the surfactant now adsorbs cooperatively onto the polymer layer. Self-assembly of surfactant molecules around the dendrimer layer will, compared to the monomeric surfactant binding at lower concentration, reduce the polymer−surfactant contact and give rise to a more viscous layer. The steeper slopes, now almost vertical, for the exposures of SDS solutions of concentrations higher than 5.5 and 6.7 mM to monolayers of PAMAM-G4 and PAMAM-G8, respectively, indicate that the surface excess does not change or changes only very slightly. This shows that the adsorbed layers are saturated with surfactant and further surfactant adsorption is unlikely due to electrostatic repulsion, although the viscoelastic properties of the system do change. In 10 mM NaCl, the reported critical micellar concentration (CMC) of SDS is 5.5 mM;[51] thus, dissipation can be attributed to the change of the viscoelastic properties of the surfactant solution above CMC,[52] as QCM-D is a very sensitive technique to bulk viscosity changes.[28]

It is also noticeable from Figure 2a,b that PAMAM-G8 shows a larger dissipation change compared to PAMAM-G4 for the highest SDS concentrations. The more irregular and thick PAMAM-G8/SDS adsorbed layers can dissipate more energy than the thinner PAMAM-G4/SDS, but the ratio $\Delta D/\Delta f$ is in both cases $\sim 5 \times 10^{-8}$, which suggests that the layers are still rigid and have a similar structure but a different composition.

dx.doi.org/10.1021/la400774p | *Langmuir* 2013, 29, 5817−5831

The corresponding experimental procedure was used for the NR measurements, which aimed to further reveal the structure and composition of the mixed adsorption layers. The exposure of SDS to the PAMAM monolayers causes notable changes in the NR profiles compared to the preadsorbed dendrimer monolayers alone, as is shown in Figures 3 and 4. The parameters from the simultaneous modeling of different isotopic contrasts of corresponding measurements and the calculated surface excesses are listed in Tables 2 and 3. Good agreement with the QCM-D measurements (Figure 2) is observed, provided that we consider the total amount of material in the interfacial layer including the water which is coupled to adsorbed molecules in such a resonance technique. Some small differences can be attributed to coupled solvent and viscoelastic effects that are especially important during the QCM-D measurements. It is noteworthy that NR data features fringes for the isotopic contrast involving hSDS/D_2O. This allows us to make some conclusions regarding the adsorbed layer structure even before the modeling below. The presence of fringes is indicative of a well-defined surface layer and allows for very accurate determination of the layer thickness. The shift of the fringe toward lower Q-vectors, as observed for PAMAM-G4 monolayers with increasing SDS concentration, shows that the layer thickness increases. Simultaneously, the peak becomes less pronounced, suggesting a more diffuse layer. The corresponding experiment in the case of the PAMAM-G8 layer features two distinct fringes, which become more pronounced as the SDS concentration increases. This shows that the PAMAM-G8/SDS layer is significantly thicker and more well-defined than the PAMAM-G4/SDS layer. The modeling of the NR data will allow us to identify the differences in layer structures in more detail.

The model that best fits the NR data shows that, at low SDS concentrations, surfactant monomers adsorb on top of the polymer layer for dendrimers of both generations. In addition, SDS also penetrates the preadsorbed dendrimer layer and causes its expansion by approximately 80% and 90% for PAMAM-G4 and PAMAM-G8, respectively, compared to the original thicknesses. Yet, the PAMAM monolayers can still be considered compact relative to their morphology in the bulk solution as the thickness remains just 50% of the dendrimer hydrodynamic diameter. The surfactant molecule is relatively small compared to the size of the dendrimer of both generations studied. In this context, it should also be noted that the dendrimer interior is relatively hydrophobic and accessible for surfactant penetration driven by hydrophobic interactions. Smith et al.[53] have shown that the association between zwitterionic lipids and PAMAM dendrimers are driven by the hydrophobic interaction between the lipid acyl chain and the interior of the dendrimer. A similar study of the interactions of preadsorbed PAMAM dendrimers on silica with DNA[33] showed that in that case the dendrimer layer remains unchanged. However, DNA is a bigger semiflexible polyelectrolyte compared to PAMAM dendrimers which could be a reason that no swelling due to penetration of the polymer was observed in that case. Wyn-Jones and et al.[13] suggested, based on their studies of the PAMAM/SDS system in bulk solution, that SDS binds at low surfactant concentrations as monomers to the dendrimers. Recently, Cheng et al.[14,54] investigated the interactions between PAMAM-G4 and SDS by ^{1}H NMR and reported that at low SDS/G4 molar ratios, SDS monomers could be present in the interior of the dendrimer. This group has also reported on the association of SDS with PAMAM generations 3, 5, and 6 dendrimers at high pH, where the surfactant acyl chain is proposed to locate in the hydrophobic pockets of the dendrimer while its headgroup localizes near the core or the terminal amine groups of the dendrimer.[55] The ability of the surfactant tail to be located in the interior of the dendrimers could also be limited for higher generations, as previous studies have shown that steric effects can block the access to the hydrophobic pockets.[55,56] The previous bulk studies and our data suggest that some of the interactions at the solid−liquid interface could be attributed to penetration of the surfactant in the hydrophobic pockets of the dendrimer adsorbed layer, although it is not possible from our measurements to identify the exact location of the surfactant headgroup and hydrophobic tail with respect to the dendrimer structure.

The adsorbed PAMAM-G4 dendrimers, modeled as a single layer, expand from roughly 13 Å to 24 Å due to interaction with SDS at low concentration (see Table 2). The adsorbed PAMAM-G8 dendrimers with SDS had to be modeled as two layers to get a good fit, in total expanding from roughly 33 Å to 63 Å. It is also possible that an additional surfactant layer can adsorb on top of the dendrimer/surfactant layer as this model gives the best fit to the experimental NR data. At low bulk surfactant concentrations, the surfactant layer on top of the PAMAM-G4 dendrimer layers is very thin (8 Å) with a high solvent content (69%). Its thickness increases to 26 Å and solvent content reduces to about 50% as the bulk surfactant concentration increases to above CMC. The same behavior is observed for the PAMAM-G8 monolayer where the surfactant layer goes from 7 to 35 Å from low to high surfactant concentration. At SDS concentrations above CMC, the thickness of the surfactant layer is larger than that of an SDS monolayer and thus its morphology must be in the form of attached aggregates or a bilayer-like structure.

Due to the known bulk structure of the dendrimers,[2] we can assume that the adsorbed layers have similar structure to half spheroids on a flat surface. For this structure, the calculated surface area for the expanded layer of PAMAM-G4 is approximately 2800 Å^2, while for PAMAM-G8 it is more than 18000 Å^2, which represents 130−200% more surface area compared to the substrate without dendrimer (additional information about the surface area calculation can be found in the Supporting Information). If we calculate the maximum number of surfactant molecules in this region for monolayer coverage, taking an SDS surface area of 25−40 Å^2, we find that PAMAM-G4 could bind a maximum of 75−120 surfactant molecules compared to approximately 450−720 for PAMAM-G8. The estimated number of surfactant molecules per dendrimer for the NR models was a maximum of 23 for PAMAM-G4 (less than a monolayer). This indicates that the layer is made up of patches of aggregates. For PAMAM-G8, the estimated number is much larger (a minimum of 1600); thus, the actual number of surfactant molecules per dendrimer exceeds the calculated amount for a monolayer, which is additional proof that the morphology is aggregates or a bilayer-like structure. The expansion of the higher generation dendrimer promotes the binding of a greater amount of surfactant due to the larger exposed surface area and promotes surfactant aggregation possibly in the form of bridges between the adsorbed dendrimer molecules. These data show that the relative expansion of the dendrimer molecule with changing amount of adsorbed surfactant depends on the degree to which the surfactant penetrates the dendrimer layer and therefore also the dendrimer generation.

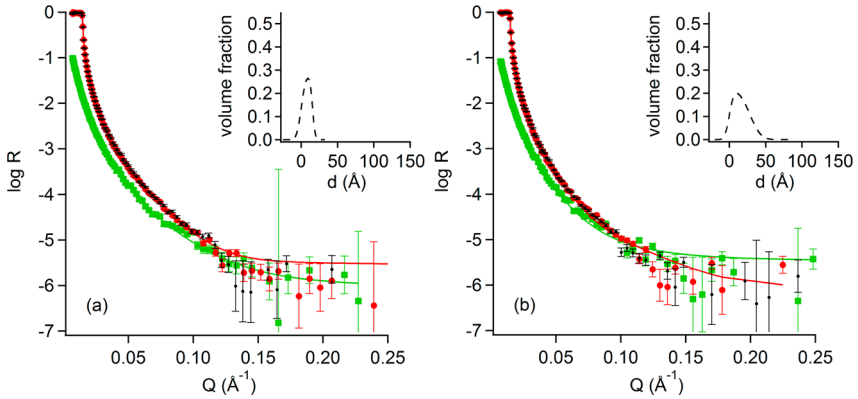

Figure 5. Neutron reflectivity profiles for rinsing with solvent after the addition of SDS on a (a) PAMAM-G4 and (b) PAMAM-G8 monolayer. The solvent contrasts used to characterize the layers were D_2O (red) and H_2O (green). The black dots correspond to the neutron reflectivity profiles before the addition of SDS for comparison. The lines correspond to the calculated model. The insets correspond to the volume fraction of dendrimer (black dashed line) as a function of the distance (d) to the surface (SiO_2).

The dendrimer molecules are highly charged on the surface but the interior amines remain mainly uncharged at this pH. Experimental results[57] and simulations of dendrimers in solution[2,50] and adsorbed on a flat surface[58] have suggested that terminal groups of PAMAM dendrimers at neutral pH could fold back to the interior of the dendrimer; thus, addition of SDS could result in a conformational change and expansion of the layer. Porus et al.[59] have reported that PAMAM dendrimers adsorbed on silica can swell in solutions of high ionic strength and low pH. For the addition of SDS, the expansion can be attributed both to a competition between the dendrimer−surface and dendrimer−surfactant interactions, decreasing the strength of the electrostatic interaction with the substrate, and to penetration of the surfactant in the dendrimer layer. Similar behavior has also been observed for PEI on mica at pH 5.7 and 10 mM NaCl.[18] Zhang et al.[19] observed that PEI adsorbs at pH 7 as a thin layer and interacts with SDS but did not observe any change of the polymer layer thickness due to the addition of the surfactant; it should, however, be noted that their work was carried out without any addition of salt. We can conclude from our NR data on the PAMAM/SDS system that expansion of the dendrimer layer after interaction with low concentrations of SDS is due to a combination of electrostatic and hydrophobic interactions with the dendrimer.

With an increased SDS concentration of 2.1 mM (and higher), both the thickness of the PAMAM-G4 layer and the solvent content in this layer decrease from 24 Å to 14 Å and from 70% to 50%, respectively, while an average of 20 surfactant molecules per dendrimer molecule are trapped in the dendrimer layer. Similar deswelling behavior has been observed for cationic polyelectrolyte brushes interacting with SDS,[24] as the dodecyl sulfate ion replaces the mobile hydroxyl counterions and reduces the osmotic pressure within the dendrimer layer. The PAMAM-G8 layer does not show deswelling at higher surfactant concentrations.

Caminati et al.[9] proposed that in the bulk solution oppositely charged dendrimer/surfactant complexes formed with dendrimers of higher generations are characterized by cooperative binding of the surfactant and closed structures. The further addition of SDS above the CMC (6.7 mM) leads to the formation of steady state surfactant aggregates or bilayer-like assemblies on the dendrimer surface with a thickness of 25−35 Å. Further increase of the bulk surfactant concentration does not cause any further changes in the layer structure. The results from our measurements could not resolve the structure or morphology of the surfactant aggregates bound to the dendrimer layer due to its larger roughness, although we note that Ottaviani et al.[10,11] suggested that PAMAM of higher generations interacts with oblate micelles or bilayers. In the latter case they proposed that the interactions result in surfactant molecules bridging different dendrimer molecules, and the hydrophobic chains of the surfactant possibly partially entering the dendrimer layer structure.

Nonequilibrium Character of the Adsorption. The reversibility of the adsorption of SDS onto the dendrimer monolayer was studied by diluting the bulk solution with a 10 mM NaCl solution (free of dendrimer and surfactant). Figure 5 shows the fitted NR profiles (after dilution) in comparison with the NR data of the initial PAMAM monolayers (prior to its exposure to surfactant). It was not necessary to include surfactant in the interfacial model after rinsing in order to get good fits to the experiment data. Furthermore, the surface excess of dendrimer after removing the surfactant by rinsing the sample cell with pure salt solution is the same to within the uncertainty of the measurements, as the preadsorbed monolayer before surfactant addition. Thus, we may infer that the surfactant adsorption onto the dendrimers is fully reversible. The layers correspond to polymer with a solvent content of 72% and 79%, which in comparison with the solvent content before the addition of SDS are changes of +7% and −5%, respectively. While the changes in these data are small, the trends are consistent with those in our QCM-D data, which show that the total surface excess of the PAMAM-G4 also changes by +17% and that of PAMAM-G8 changes by −9% in comparison with the initial dendrimer monolayer prior to the surfactant addition (see comparison of full and dashed line arrows in Figure 2). These qualitatively consistent data from the two techniques imply that exposure to the surfactant has resulted in lasting minor structural changes to the dendrimer layer.

We may compare the PAMAM dendrimer adsorption with previous studies on behavior for the branched PEI. Zhang et al.[19] observed that the reversibility of the surfactant adsorption to PEI monolayers on hydrophilic silica depends on the solution pH. At pH 2.4, PEI adsorbs as a thick layer and the adsorption of SDS causes further swelling of the polymer. The surfactant adsorption process is irreversible, as dilution does

dx.doi.org/10.1021/la400774p | *Langmuir* 2013, 29, 5817−5831

not cause desorption of the surfactant. At pH 7 and 10, PEI adsorbs as a thin layer, and surfactant adsorption is reversible at pH 7, but not at pH 10 where the surfactant molecules irreversibly penetrate the polymer layer. We have shown that PAMAM dendrimers also adsorb as thin, compacted layers to hydrophilic silica at pH 7, but, unlike for PEI, the adsorbed layers swell when they interact with the oppositely charged surfactant and the process appears to be reversible. We attribute the reversible expansion of the dendrimer layer upon surfactant binding to the monodisperse and hierarchical structure of the dendrimer molecule which is missing for PEI. This characteristic points to potential applications where well-defined responsive surfaces are needed.

Interaction of Premixed PAMAM/SDS Samples with Hydrophilic Silica. In looking at dendrimer−surfactant interactions at surfaces in the preadsorbed case above, we learned that the dendrimer adsorbs as a compact monolayer, that surfactant monomers then aggregates bind to and penetrate the dendrimer layer resulting in its expansion, and that surfactant adsorption is reversible. One of the important aspects of this study is to reveal the effects of the bulk aggregates on the adsorption process. For this purpose, we now compare the results above with those from the adsorption of PAMAM/SDS mixtures preformed in the bulk. For this work, we focus on the PAMAM-G4/SDS system due to limitations in beam time, and also because the PAMAM-G4 dendrimer structure is better defined.

The importance of the electrostatic interactions between oppositely charged polyelectrolyte/surfactant mixtures has been highlighted above. In order to understand the interaction of bulk dendrimer/surfactant complexes and aggregates with a solid surface we need to know their charge with respect to the bulk composition. Figure 6 shows the EM data from positive to

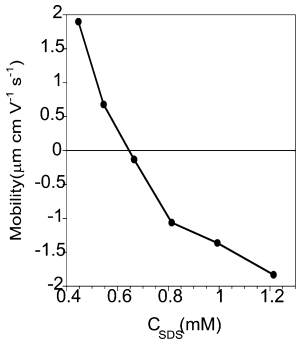

Figure 6. Electrophoretic mobility of dendrimer/SDS complexes for 100 ppm PAMAM-G4 as a function of the bulk SDS concentration. Lines are only to guide the eye.

negative PAMAM-G4/SDS complexes. The point of charge neutrality for the bulk concentrations of dendrimers stated above corresponds to a concentration of 0.66 mM SDS.

We employed both QCM-D and NR to characterize the adsorption of PAMAM-G4/SDS mixtures at the hydrophilic silica−water interface. Figure 7 shows the surface excess determined by QCM-D of single direct additions of PAMAM-G4/SDS mixtures at different bulk concentrations of SDS. The dashed vertical line corresponds to the concentration of surfactant where the complexes have neutral charge. For SDS concentrations below the charge neutrality point, the surface excess increases with the surfactant concentration. This is not surprising since the complexes

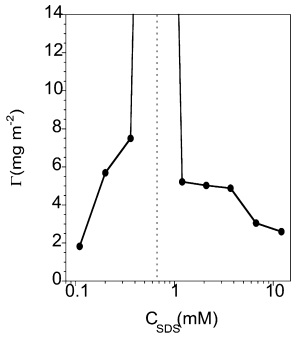

Figure 7. Surface excess (Γ) of layers of PAMAM-G4/SDS mixtures on silica obtained from modeling of the QCM-D data. The dashed line corresponds to the concentration where the complexes have neutral charge. Lines are only to guide the eye.

have a net positive charge, and thus the adsorption is favored due to electrostatic attractive interactions with the negatively charged silica. For dendrimer/surfactant mixtures around the charge neutrality point, macroscopic phase separation is observed as expected for strongly associating polyelectrolyte/surfactant systems.[15] Under these conditions, the QCM-D measurements give large surface excess values, beyond the detection limits of the instrument. We attribute the large surface excesses to the precipitation and sedimentation of bulk aggregates as evidenced by a white precipitate on the crystals after the experiment. Note that, unlike the QCM-D sensors, NR cells used in this study have the silica substrate above the liquid; thus, deposition of material due to precipitation and sedimentation that would obscure the signal from adsorption of complexes is avoided. These results are consistent with the findings of recent work linking the interfacial properties of a different strongly interacting P/S mixture to the creaming or sedimentation of bulk aggregates under gravity depending on the location of the probed interface with respect to the bulk liquid.[60] Above the charge neutrality point (i.e., negatively charged bulk complexes), the surface excess decreases as the bulk surfactant concentration increases. This observation can be rationalized in terms of the excess of surfactant molecules present in the bulk complexes which reduced their affinity for adsorption to hydrophilic silica. Similar behavior has been observed not only for the adsorption of PEI/SDS mixtures[21] at the silica/water interface, but also for the adsorption of mixtures of nonionic polymers and SDS on silica.[61,62] The total adsorbed amount here increases as a function of the surfactant concentration and has a maximum below the critical association concentration of SDS above which it then decreases.

In the NR measurements, premixed solutions of 100 ppm PAMAM-G4 and surfactant at only two charge ratios were each exposed to hydrophilic silica surfaces: charge neutrality (0.66 mM SDS) and negatively charged (2.1 mM SDS). The experimental NR profiles of the mixtures of different isotopic contrasts and the calculated curves from the model fits to them are shown in Figure 8. Immediately it can be observed that the reflectivity profiles for the two charge ratios show very different features. The mixtures corresponding to negatively charged complexes present a very distinct fringe for the contrast involving hSDS/D_2O around a momentum transfer of 0.05 $Å^{-1}$, while for the reflectivity profile for the equivalent contrast at charge neutrality this fringe is hardly visible.

Table 4 shows the parameters employed for fitting the layer models to data recorded for the PAMAM-G4/SDS mixtures.

dx.doi.org/10.1021/la400774p | Langmuir 2013, 29, 5817−5831

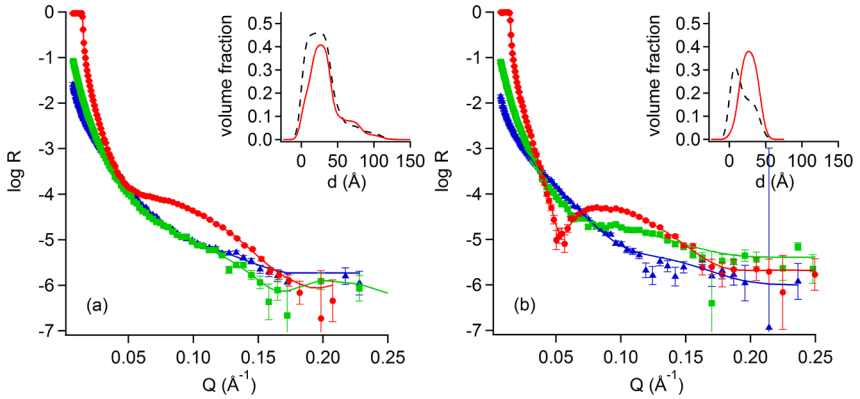

Figure 8. Neutron reflectivity profiles for the adsorption of PAMAM-G4/SDS mixtures on silica, for 100 ppm G4 and (a) 0.66 and (b) 2.1 mM SDS. The solvent contrasts used to characterize the layers were hSDS/D_2O (red), dSDS/H_2O (green), and dSDS/cmSi (blue). The lines correspond to the calculated model. The insets correspond to the volume fraction of dendrimer (black dashed line) and surfactant (red line) as a function of the distance (d) to the surface (SiO_2).

Table 4. Parameters Obtained from the Modeling of the NR Profiles, Calculated Total Mass (m_{total}), and Number of Surfactant Molecules Per Polymer Molecule for the Adsorption of PAMAM-G4/SDS Mixtures on Silica[a]

C_{SDS} (mM)	layers	d (Å)	δ (Å)	$v_{dendrimer}$	$v_{surfactant}$	$n_{surfactant}/n_{dendrimer}$	m_{total} (mg m^{-2})
0.66	Layer 1	14.0 ± 0.5	5 ± 2	0.45 ± 0.01	0.20 ± 0.03	21 ± 3	11.7 ± 0.1
	Layer 2	26 ± 1	5 ± 1	0.46 ± 0.01	0.41 ± 0.06	43 ± 5	
	Layer 3	13.9 ± 0.6	6 ± 3	0.16 ± 0.01	0.11 ± 0.03	33 ± 8	
	Layer 4	28 ± 2	6 ± 3	0.06 ± 0.01	0.08 ± 0.03	62 ± 22	
	Layer 5	28 ± 2	9 ± 3	0.03 ± 0.01	0.02 ± 0.01	31 ± 1	
2.1	Layer 1	13.2 ± 0.3	6 ± 3	0.37 ± 0.02	0.04 ± 0.01	6 ± 1	4.6 ± 0.2
	Layer 2	29 ± 2	7 ± 2	0.17 ± 0.01	0.39 ± 0.03	112 ± 9	

[a]The parameters are described in the footnote of Table 2.

For the mixture at charge neutrality, a five-layer model on silica was required to obtain good fits to data from all three isotopic contrasts, whereas the results for the sample with negatively charged complexes could be fitted with a two-layer model. For the charge neutral mixtures, the first layer, closest to the silica, was composed of a 29% higher volume fraction of dendrimer compared to the preadsorbed case. This could possibly be explained by a lower charge of the complexes, which decreases the intermolecular electrostatic repulsive interaction. It has previously been shown that screening the electrostatic interaction by, e.g., salt might lead to a higher adsorbed amount of the polymer as intermolecular electrostatic repulsive interactions often limit the adsorption of oppositely charged polymers on surfaces.[63] The volume fraction adsorbed to silica of other polymers, such as Pluronic F108, has also been shown to increase by adsorbing it as a complex with SDS.[64] These results are relevant for the present study where we wish to control the adsorbed dendrimer structure.

PAMAM dendrimers have a high affinity for the surface; therefore, the dendrimers in the mixture compete to interact with the substrate and the surfactant. It has been shown that the mixing process has a large effect on the charge and size distribution of aggregates formed in polyelectrolyte/surfactant mixtures.[35] The film structures and composition vary greatly if we compare the data from the premixed experiment to those from the preadsorbed experiment. Therefore, polymer/surfactant interactions and aggregation phenomena in the bulk, which leads to the formation of kinetically trapped aggregates, clearly influence the mixed layers on the surface.

For negatively charged complexes, both layers contain polymer and surfactant. The total surface excess from NR (4.6 ± 0.2 mg m^{-2}) matches to a difference of just 12% with that measured using QCM-D (5.2 ± 0.1 mg m^{-2}). In the layer closest to the substrate the number of surfactant molecules per dendrimer molecule is low (6) compared to the preadsorbed maximum case (~20), which makes this layer positively charged (Table 4). The outermost layer has over 100 surfactant molecules per dendrimer molecule, which gives a net negative surface charge inhibiting multilayer formation. At higher surfactant concentrations, the surface excess is reduced, as has been observed PCMA/SDS mixtures.[65]

Pathway Dependence of PAMAM/SDS Interactions with Hydrophilic Silica. To estimate the applicability of a thermodynamic model to the experimental data in the present work, we investigated the effect of the adsorption pathway, i.e., sequential injections of samples with increasing SDS concentration vs a single direct addition. If a system that has reached steady state is in true equilibrium, then the nature of the adsorbed layer should be independent of the sample history. As above, these measurements were carried out with PAMAM-G4 and PAMAM-G8 for preadsorbed layers and with PAMAM-G4/SDS mixtures for the premixed case.

Figure 9 shows the surface excess determined by QCM-D measurements for different concentrations of SDS interacting with preadsorbed PAMAM monolayers of generations 4 and 8 on hydrophilic silica for both the direct (red) and sequential (black) addition methods employed. For dendrimers of both generations, it is clear that the surface excess is the same to within 20%, regardless of whether the SDS concentration was increased sequentially or the final concentration was exposed to the monolayer directly. Therefore, we can conclude that the system is at equilibrium and that thermodynamic models, such

dx.doi.org/10.1021/la400774p | Langmuir 2013, 29, 5817−5831

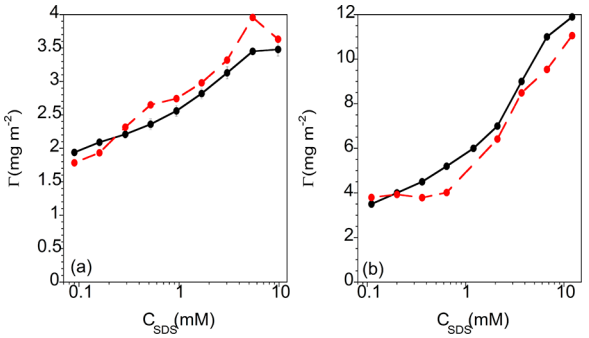

Figure 9. Surface excess (Γ) of layers of SDS interacting with preadsorbed PAMAM (a) G4 and (b) G8 monolayers on silica obtained from modeling of the QCM-D data. The addition of SDS was performed sequentially (black) and directly (red). Lines are only to guide the eye.

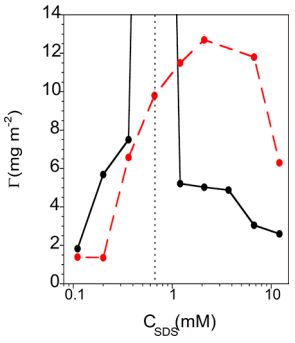

Figure 10. Surface excess (Γ) of layers of PAMAM-G4/SDS mixtures on silica obtained from modeling of the QCM-D data. The addition of SDS was performed sequentially (red) and separately (black). In the latter case the data are repeated from Figure 7 for clarity. Lines are only to guide the eye.

as the self-consistent field lattice model,[66] could be applied to these experimental data. Dendrimer adsorption onto planar surfaces have been previously simulated using lattice models,[48] along with the complexation between oppositely charged P/S systems,[67] so future theoretical work could be compared with the experimental data presented here.

The results are quite different for adsorption from mixtures of PAMAM-G4/SDS, as is obvious from Figure 10. As we saw above, the experiments where the exposure of premixed bulk complexes and aggregates to hydrophilic silica was performed in single direct additions, the maximum adsorption is around the point of charge neutrality of the bulk complexes, i.e., in the two-phase region. Under these conditions sedimentation takes place, and therefore the sensed mass with QCM-D is large. For the sequential addition of different mixtures, from low to high concentrations of SDS, the adsorption has a maximum at concentrations above the charge neutrality of the complexes, at a surfactant concentration above 2 mM. The surface excess of the mixtures with positively charged complexes is lower for the sequential additions than for the direct addition, but the situation is reversed for negatively charged complexes. The pathway dependence shows that this system has not reached equilibrium. In fact, we cannot determine which approach is closer to the true equilibrium of the system. Similar observations have been made for PCMA/SDS mixtures.[27] These results agree with previous findings where adsorption occurs due to a transport mechanism of the bulk complexes in the phase separation region of the polyelectrolyte/surfactant mixture.[60] The exposure of the surface to the bulk complexes through different pathways of adsorption generates different trapped adsorbed layers; as for the single direct addition case, more material could be precipitated on the crystals which could be washed away for the sequential additions. These findings indicate that such data are likely to be far from equilibrium and should not be used to validate thermodynamic models.

CONCLUSIONS

Cationic PAMAM dendrimers of generations 4 and 8 adsorb irreversibly to hydrophilic silica at pH 7 in 10 mM NaCl as a very compact monolayer with high solvent content. The consequences of the interaction of the anionic surfactant SDS with PAMAM monolayers in terms of the structure, composition, and viscoelastic properties of the layers can be controlled by varying the concentration of SDS and dendrimer generation. At low SDS concentrations, surfactant binds to the polymer in monomeric form, driven by a combination of electrostatic interactions and hydrophobic interactions between the surfactant tail and the relatively hydrophobic interior of the dendrimer. The adsorption of surfactant in this concentration range causes expansion of the polymer layer. The effect is larger for PAMAM-G8 than for PAMAM-G4, since the PAMAM-G8 provides a larger effective surface area that promotes the binding of a higher number of surfactant molecules. The surfactant binds cooperatively to the dendrimers at higher concentrations of SDS, leading to the formation of surfactant aggregates or a bilayer-like structure on the polymer layer. The adsorption of surfactant is reversible upon dilution. However, exposure to surfactant produces minor lasting structural changes on the preadsorbed PAMAM monolayers, while the surface excess of polymer does not change.

We have shown that the bulk interactions have a great effect on the interfacial layers, as adsorption of premixed PAMAM/SDS samples is markedly different from the sequential adsorption of surfactant to a preformed dendrimer layer. The interfacial layer is now determined by the balance between dendrimer−surface and complex−surface electrostatic interactions. For positively charged complexes the adsorption increases as the surfactant concentration increases and formation of thick multilayer occurs around the charge neutrality of the complexes. At charge neutrality the complexes phase separate and precipitate, and this leads to very high surface excess due to sedimentation only if the probed interface is located under the bulk liquid. It is therefore critical that one considers carefully the geometry of the system to separate sedimentation from adsorption. For negatively charged complexes the surface excess decreases as the surfactant concentration increases as a result of electrostatic repulsion.

The question of whether PAMAM/SDS interfacial structures investigated in this work have reached chemical equilibrium or not was determined by investigating equivalent systems with respect to different experimental pathways. The surface excess is equivalent for SDS interacting with preadsorbed PAMAM monolayers if the adsorption is performed in sequential additions of different concentrations of SDS or a single direct addition. In contrast, for premixed solutions the pathway of adsorption changes the surface excess indicating that non-equilibrium effects in the bulk have a profound effect on the interfacial properties. These results show that the application of a thermodynamic model to the experimental data would be appropriate in the former case, but not in the latter case where

dx.doi.org/10.1021/la400774p | Langmuir 2013, 29, 5817−5831

details of the sample history are critically important in determining the surface properties.

Dendrimers have been shown to be good candidates for the delivery of small molecules as well as macromolecules to interfaces. The advantage of the dendrimer molecular architecture is that we can utilize both the hydrophobic and the attractive electrostatic interaction to capture amphiphilic molecules. The present work shows that both the dendrimer generation and the route of delivery can be used to control the amount of material delivered. The surface properties can also be tuned by utilizing the nonequilibrium effects in the bulk. Insight from these findings on well-defined model polyelectrolytes can help to optimize the use of hyperbranched polymers in applications in consumer products and nanomaterials.

■ ASSOCIATED CONTENT

Supporting Information

Voigt model description, characterization of the silica layers, QCM-D frequency and dissipation versus time plot and dendrimer surface area calculations. This material is available free of charge via the Internet at http://pubs.acs.org.

■ AUTHOR INFORMATION

Corresponding Author

*E-mail: Marianna.Yanez@fkem1.lu.se.

Notes

The authors declare no competing financial interest.

■ ACKNOWLEDGMENTS

This work was supported by the Swedish Research Council (VR) through the Linnaeus grant Organizing Molecular Matter (OMM) center of excellence (239-2009-6794). The Knut and Alice Wallenberg foundation funded the acquisition of the QCM-D instrument. We thank the ILL for beam time allocations on FIGARO and Bob Thomas for helpful discussions.

■ REFERENCES

(1) Tomalia, D. A.; Baker, H.; Dewald, J.; Hall, M.; Kallos, G.; Martin, S.; Roeck, J.; Ryder, J.; Smith, P. A New Class of Polymers: Starburst-Dendritic Macromolecules. *Polym. J.* **1985**, *17* (1), 117−132.

(2) Maiti, P. K.; Çagın, T.; Wang, G.; Goddard, W. A. Structure of PAMAM Dendrimers: Generations 1 through 11. *Macromolecules* **2004**, *37* (16), 6236−6254.

(3) Li, T.; Hong, K.; Porcar, L.; Verduzco, R.; Butler, P. D.; Smith, G. S.; Liu, Y.; Chen, W.-R. Assess the Intramolecular Cavity of a PAMAM Dendrimer in Aqueous Solution by Small-Angle Neutron Scattering. *Macromolecules* **2008**, *41* (22), 8916−8920.

(4) Cakara, D.; Kleimann, J.; Borkovec, M. Microscopic Protonation Equilibria of Poly(amidoamine) Dendrimers from Macroscopic Titrations. *Macromolecules* **2003**, *36* (11), 4201−4207.

(5) Esfand, R.; Tomalia, D. A. Poly(amidoamine) (PAMAM) dendrimers: from biomimicry to drug delivery and biomedical applications. *Drug Discovery Today* **2001**, *6* (8), 427−436.

(6) Wang, Y.; Boros, P.; Liu, J.; Qin, L.; Bai, Y.; Bielinska, A. U.; Kukowska-Latallo, J. F.; Baker, J. R.; Bromberg, J. S. DNA/Dendrimer Complexes Mediate Gene Transfer into Murine Cardiac Transplants ex Vivo. *Mol. Ther.* **2000**, *2* (6), 602−608.

(7) Shen, L.; Hu, N. Heme protein films with polyamidoamine dendrimer: direct electrochemistry and electrocatalysis. *Biochim. Biophys. Acta, Bioenerg.* **2004**, *1608* (1), 23−33.

(8) Moorefield, C. N.; Newkome, G. R. Unimolecular micelles: supramolecular use of dendritic constructs to create versatile molecular containers. *C. R. Chim.* **2003**, *6* (8−10), 715−724.

(9) Caminati, G.; Turro, N. J.; Tomalia, D. A. Photophysical investigation of starburst dendrimers and their interactions with anionic and cationic surfactants. *J. Am. Chem. Soc.* **1990**, *112* (23), 8515−8522.

(10) Ottaviani, M. F.; Turro, N. J.; Jockusch, S.; Tomalia, D. A. Aggregational process of the positively charged surfactants CTAC and CAT16 in the presence of starburst dendrimers: an electron paramagnetic resonance spectroscopic study. *Colloids Surf., A* **1996**, *115* (0), 9−21.

(11) Ottaviani, M. F.; Andechaga, P.; Turro, N. J.; Tomalia, D. A. Model for the Interactions between Anionic Dendrimers and Cationic Surfactants by Means of the Spin Probe Method. *J. Phys. Chem. B* **1997**, *101* (31), 6057−6065.

(12) Ottaviani, M.; Daddi, R.; Brustolon, M.; Turro, N.; Tomalia, D. Interaction between Starburst Dendrimers and SDS micelles studied by continuous-wave and pulsed electron spin resonances. *Appl. Magn. Reson.* **1997**, *13* (3), 347−363.

(13) Sidhu, J.; Bloor, D. M.; Couderc-Azouani, S.; Penfold, J.; Holzwarth, J. F.; Wyn-Jones, E. Interactions of Poly(amidoamine) Dendrimers with the Surfactants SDS, DTAB, and C12EO6: An Equilibrium and Structural Study Using a SDS Selective Electrode, Isothermal Titration Calorimetry, and Small Angle Neutron Scattering. *Langmuir* **2004**, *20* (21), 9320−9328.

(14) Fang, M.; Cheng, Y.; Zhang, J.; Wu, Q.; Hu, J.; Zhao, L.; Xu, T. New Insights into Interactions between Dendrimers and Surfactants. 4. Fast-Exchange/Slow-Exchange Transitions in the Structure of Dendrimer−Surfactant Aggregates. *J. Phys. Chem. B* **2010**, *114* (18), 6048−6055.

(15) Holmberg, K.; Jönsson, B.; Krongberg, B.; Lindman, B. *Surfactants and Polymers in Aqueous Solution*, 2nd ed.; John Wiley & Sons, LTD: England, 2007; pp 299−302.

(16) Shubin, V.; Petrov, P.; Lindman, B. The effect of surfactants on adsorbed layers of a cationic polyelectrolyte. *Colloid Polym. Sci.* **1994**, *272* (12), 1590−1601.

(17) Penfold, J.; Tucker, I.; Staples, E.; Thomas, R. K. Manipulation of the Adsorption of Ionic Surfactants onto Hydrophilic Silica Using Polyelectrolytes. *Langmuir* **2004**, *20* (17), 7177−7182.

(18) Dedinaite, A.; Mészaros, R.; Claesson, P. M. Effect of Sodium Dodecyl Sulfate on Adsorbed Layers of Branched Polyethylene Imine. *J. Phys. Chem. B* **2004**, *108* (31), 11645−11653.

(19) Zhang, X.; Taylor, D.; Thomas, R.; Penfold, J.; Tucker, I. Modifying the Adsorption Properties of Anionic Surfactants onto Hydrophilic Silica Using the pH Dependence of the Polyelectrolytes PEI, Ethoxylated PEI, and Polyamines. *Langmuir* **2011**, *27* (7), 3569−3577.

(20) Varga, I.; Mezei, A.; Meszaros, R.; Claesson, P. M. Controlling the interaction of poly(ethylene imine) adsorption layers with oppositely charged surfactant by tuning the structure of the preadsorbed polyelectrolyte layer. *Soft Matter* **2011**, *7* (22), 10701−10712.

(21) Mészáros, R.; Thompson, L.; Varga, I.; Gilányi, T. Adsorption Properties of Polyethyleneimine on Silica Surfaces in the Presence of Sodium Dodecyl Sulfate. *Langmuir* **2003**, *19* (23), 9977−9980.

(22) Penfold, J.; Tucker, I.; Thomas, R. K. Polyelectrolyte Modified Solid Surfaces: the Consequences for Ionic and Mixed Ionic/Nonionic Surfactant Adsorption. *Langmuir* **2005**, *21* (25), 11757−11764.

(23) Plunkett, M. A.; Claesson, P. M.; Rutland, M. W. Adsorption of a Cationic Polyelectrolyte followed by Surfactant-Induced Swelling, Studied with a Quartz Crystal Microbalance. *Langmuir* **2002**, *18* (4), 1274−1280.

(24) Moglianetti, M.; Webster, J. R. P.; Edmondson, S.; Armes, S. P.; Titmuss, S. A Neutron Reflectivity Study of Surfactant Self-Assembly in Weak Polyelectrolyte Brushes at the Sapphire−Water Interface. *Langmuir* **2011**, *27* (8), 4489−4496.

(25) Rojas, O. J.; Neuman, R. D.; Claesson, P. M. Desorption of Low-Charge-Density Polyelectrolyte Adlayers in Aqueous Sodium n-Dodecyl Sulfate Solution. *J. Colloid Interface Sci.* **2001**, *237* (1), 104−111.

(26) Nylander, T.; Samoshina, Y.; Lindman, B. Formation of polyelectrolyte−surfactant complexes on surfaces. *Adv. Colloid Interface Sci.* **2006**, *123−126* (0), 105−123.
(27) Dedinaite, A.; Claesson, P. M.; Bergström, M. Polyelectrolyte−Surfactant Layers: Adsorption of Preformed Aggregates versus Adsorption of Surfactant to Preadsorbed Polyelectrolyte. *Langmuir* **2000**, *16* (12), 5257−5266.
(28) Höök, F.; Kasemo, B.; Nylander, T.; Fant, C.; Sott, K.; Elwing, H. Variations in Coupled Water, Viscoelastic Properties, and Film Thickness of a Mefp-1 Protein Film during Adsorption and Cross-Linking: A Quartz Crystal Microbalance with Dissipation Monitoring, Ellipsometry, and Surface Plasmon Resonance Study. *Anal. Chem.* **2001**, *73* (24), 5796−5804.
(29) Fragneto-Cusani, G. Neutron reflectivity at the solid/liquid interface: examples of applications in biophysics. *J. Phys.: Condens. Matter* **2001**, *13* (21), 4973−4989.
(30) Campbell, R. A.; Yanez Arteta, M.; Angus-Smyth, A.; Nylander, T.; Varga, I. Effects of Bulk Colloidal Stability on Adsorption Layers of Poly(diallyldimethylammonium Chloride)/Sodium Dodecyl Sulfate at the Air−Water Interface Studied by Neutron Reflectometry. *J. Phys. Chem. B* **2011**, *115* (51), 15202−15213.
(31) Ainalem, M.-L.; Carnerup, A. M.; Janiak, J.; Alfredsson, V.; Nylander, T.; Schillen, K. Condensing DNA with poly(amido amine) dendrimers of different generations: means of controlling aggregate morphology. *Soft Matter* **2009**, *5* (11), 2310−2320.
(32) Betley, T. A.; Banaszak Holl, M. M.; Orr, B. G.; Swanson, D. R.; Tomalia, D. A.; Baker, J. R. Tapping Mode Atomic Force Microscopy Investigation of Poly(amidoamine) Dendrimers: Effects of Substrate and pH on Dendrimer Deformation. *Langmuir* **2001**, *17* (9), 2768−2773.
(33) Ainalem, M.-L.; Campbell, R. A.; Nylander, T. Interactions between DNA and Poly(amido amine) Dendrimers on Silica Surfaces. *Langmuir* **2010**, *26* (11), 8625−8635.
(34) Tonigold, K.; Varga, I.; Nylander, T.; Campbell, R. A. Effects of Aggregates on Mixed Adsorption Layers of Poly(ethylene imine) and Sodium Dodecyl Sulfate at the Air/Liquid Interface. *Langmuir* **2009**, *25* (7), 4036−4046.
(35) Mezei, A.; Mészáros, R.; Varga, I.; Gilányi, T. Effect of Mixing on the Formation of Complexes of Hyperbranched Cationic Polyelectrolytes and Anionic Surfactants. *Langmuir* **2007**, *23* (8), 4237−4247.
(36) Rodahl, M.; Hook, F.; Krozer, A.; Brzezinski, P.; Kasemo, B. Quartz crystal microbalance setup for frequency and Q-factor measurements in gaseous and liquid environments. *Rev. Sci. Instrum.* **1995**, *66* (7), 3924−3930.
(37) Voinova, M. V.; Rodahl, M.; Jonson, M.; Kasemo, B. Viscoelastic Acoustic Response of Layered Polymer Films at Fluid-Solid Interfaces: Continuum Mechanics Approach. *Phys. Scr.* **1999**, *59* (5), 391.
(38) Johannsmann, D. Studies of Viscoelasticity with the QCM Piezoelectric Sensors. In Steinem, C.; Janshoff, A., Eds.; Springer: Berlin, 2007; Vol. 5, pp 49−109.
(39) Paul, S.; Paul, D.; Basova, T.; Ray, A. K. Studies of Adsorption and Viscoelastic Properties of Proteins onto Liquid Crystal Phthalocyanine Surface Using Quartz Crystal Microbalance with Dissipation Technique. *J. Phys. Chem. C* **2008**, *112* (31), 11822−11830.
(40) Campbell, R.; Wacklin, H.; Sutton, I.; Cubitt, R.; Fragneto, G. FIGARO: The new horizontal neutron reflectometer at the ILL. *Eur. Phys. J. Plus* **2011**, *126* (11), 1−22.
(41) McDermott, D. C.; Lu, J. R.; Lee, E. M.; Thomas, R. K.; Rennie, A. R. Study of the adsorption from aqueous solution of hexaethylene glycol monododecyl ether on silica substrates using the technique of neutron reflection. *Langmuir* **1992**, *8* (4), 1204−1210.
(42) Nelson, A. Co-refinement of multiple-contrast neutron/X-ray reflectivity data using MOTOFIT. *J. Appl. Crystallogr.* **2006**, *39* (2), 273−276.
(43) Abeles, F. Sur la propagation des ondes electromagnetiques dans les milieux stratifies. *Ann. Phys. (Paris, Fr.)* **1948**, *3* (4), 504−520.
(44) Maiti, P. K.; Çagın, T.; Lin, S.-T.; Goddard, W. A. Effect of Solvent and pH on the Structure of PAMAM Dendrimers. *Macromolecules* **2005**, *38* (3), 979−991.
(45) Pericet-Camara, R.; Papastavrou, G.; Borkovec, M. Atomic Force Microscopy Study of the Adsorption and Electrostatic Self-Organization of Poly(amidoamine) Dendrimers on Mica. *Langmuir* **2004**, *20* (8), 3264−3270.
(46) Bliznyuk, V. N.; Rinderspacher, F.; Tsukruk, V. V. On the structure of polyamidoamine dendrimer monolayers. *Polymer* **1998**, *39* (21), 5249−5252.
(47) Longtin, R. m.; Maroni, P.; Borkovec, M. Transition from Completely Reversible to Irreversible Adsorption of Poly(amido amine) Dendrimers on Silica. *Langmuir* **2009**, *25* (5), 2928−2934.
(48) Mansfield, M. L. Surface adsorption of model dendrimers. *Polymer* **1996**, *37* (17), 3835−3841.
(49) Böcking, T.; Wong, E. L. S.; James, M.; Watson, J. A.; Brown, C. L.; Chilcott, T. C.; Barrow, K. D.; Coster, H. G. L. Immobilization of dendrimers on Si−C linked carboxylic acid-terminated monolayers on silicon(111). *Thin Solid Films* **2006**, *515* (4), 1857−1863.
(50) Chen, W.; Tomalia, D. A.; Thomas, J. L. Unusual pH-Dependent Polarity Changes in PAMAM Dendrimers: Evidence for pH-Responsive Conformational Changes. *Macromolecules* **2000**, *33* (25), 9169−9172.
(51) Newbery, J. E. The variation of the critical micelle concentration of sodium dodecyl sulphate with ionic strength monitored by selective-ion membrane electrodes. *Colloid Polym. Sci.* **1979**, *257* (7), 773−775.
(52) Kushner, L. M.; Duncan, B. C.; Hoffman, J. I. A viscometric study of the micelles of sodium dodecyl sulfate in dilute solutions. *J. Res. Natl. Bur. Stand. (U. S.)* **1952**, *49* (2), 85−90.
(53) Smith, P. E. S.; Brender, J. R.; Dürr, U. H. N.; Xu, J.; Mullen, D. G.; Banaszak Holl, M. M.; Ramamoorthy, A. Solid-State NMR Reveals the Hydrophobic-Core Location of Poly(amidoamine) Dendrimers in Biomembranes. *J. Am. Chem. Soc.* **2010**, *132* (23), 8087−8097.
(54) Yang, K.; Cheng, Y.; Feng, X.; Zhang, J.; Wu, Q.; Xu, T. Insights into the Interactions between Dendrimers and Multiple Surfactants: 5. Formation of Miscellaneous Mixed Micelles Revealed by a Combination of 1H NMR, Diffusion, and NOE Analysis. *J. Phys. Chem. B* **2010**, *114* (21), 7265−7273.
(55) Cheng, Y.; Li, Y.; Wu, Q.; Xu, T. New Insights into the Interactions between Dendrimers and Surfactants by Two Dimensional NOE NMR Spectroscopy. *J. Phy. Chem. B* **2008**, *112* (40), 12674−12680.
(56) Watkins, D. M.; Sayed-Sweet, Y.; Klimash, J. W.; Turro, N. J.; Tomalia, D. A. Dendrimers with Hydrophobic Cores and the Formation of Supramolecular Dendrimer−Surfactant Assemblies. *Langmuir* **1997**, *13* (12), 3136−3141.
(57) Wu, B.; Li, X.; Do, C.; Kim, T.-H.; Shew, C.-Y.; Liu, Y.; Yang, J.; Hong, K.; Porcar, L.; Chen, C.-Y.; Liu, E. L.; Smith, G. S.; Herwig, K. W.; Chen, W.-R. Spatial distribution of intra-molecular water and polymeric components in polyelectrolyte dendrimers revealed by small angle scattering investigations. *J. Chem. Phys.* **2011**, *135* (14), 144903.
(58) Suman, B.; Kumar, S. Adsorption of charged dendrimers: A brownian dynamics study. *J. Phys. Chem. B* **2007**, *111* (30), 8728−8739.
(59) Porus, M.; Clerc, F.; Maroni, P.; Borkovec, M. Ion-Specific Responsiveness of Polyamidoamine (PAMAM) Dendrimers Adsorbed on Silica Substrates. *Macromolecules* **2012**, *45* (9), 3919−3927.
(60) Campbell, R. A.; Yanez Arteta, M.; Angus-Smyth, A.; Nylander, T.; Varga, I. Multilayers at Interfaces of an Oppositely Charged Polyelectrolyte/Surfactant System Resulting from the Transport of Bulk Aggregates under Gravity. *J. Phys. Chem. B* **2012**, *116* (27), 7981−7990.
(61) Berglund, K. D.; Przybycien, T. M.; Tilton, R. D. Coadsorption of Sodium Dodecyl Sulfate with Hydrophobically Modified Nonionic Cellulose Polymers. 1. Role of Polymer Hydrophobic Modification. *Langmuir* **2003**, *19* (7), 2705−2713.
(62) Berglund, K. D.; Przybycien, T. M.; Tilton, R. D. Coadsorption of Sodium Dodecyl Sulfate with Hydrophobically Modified Nonionic

Cellulose Polymers. 2. Role of Surface Selectivity in Adsorption Hysteresis. *Langmuir* **2003**, *19* (7), 2714−2721.
(63) Samoshina, Y.; Nylander, T.; Shubin, V.; Bauer, R.; Eskilsson, K. Equilibrium aspects of polycation adsorption on silica surface: How the adsorbed layer responds to changes in bulk solution. *Langmuir* **2005**, *21* (13), 5872−5881.
(64) Braem, A. D.; Biggs, S.; Prieve, D. C.; Tilton, R. D. Control of Persistent Nonequilibrium Adsorbed Polymer Layer Structure by Transient Exposure to Surfactants. *Langmuir* **2003**, *19* (7), 2736−2744.
(65) Dedinaite, A.; Claesson, P. M. Interfacial Properties of Aggregates Formed by Cationic Polyelectrolyte and Anionic Surfactant. *Langmuir* **1999**, *16* (4), 1951−1959.
(66) Fleer, G. J.; Scheutjens, J. Adsorption of interacting oligomers and polymers at an interface. *Adv. Colloid Interface Sci.* **1982**, *16*, 341−359.
(67) Wallin, T.; Linse, P. Polyelectrolyte-induced micellization of charged surfactants. Calculations based on a self-consistent field lattice model. *Langmuir* **1998**, *14* (11), 2940−2949.